Vibrational Spectroscopy of 1,1-Difluorocyclopropane-d_0, -d_2, and -d_4: The Equilibrium Structure of Difluorocyclopropane

Norman C. Craig,*,† David Feller,‡ Peter Groner,§ Hong Yuan Hsin,† Donald C. McKean,|| and Deacon J. Nemchick†

Department of Chemistry and Biochemistry, Oberlin College, Oberlin, Ohio 44074, Department of Chemistry, Washington State University, Pullman, Washington 99164-4630, Department of Chemistry, University of Missouri-Kansas City, Kansas City, Missouri 64110-2499, and School of Chemistry, University of Edinburgh, Edinburgh EH9 3JJ, United Kingdom

Received: December 18, 2006; In Final Form: January 31, 2007

IR and Raman spectra are reported for 1,1-difluorocyclopropane-d_0, -d_2, and -d_4, and complete assignments of vibrational fundamentals are given for these species. These assignments are consistent with predictions of frequencies, intensities, and Raman depolarization ratios computed with the B3LYP/cc-pVTZ quantum chemical (QC) model. Ground state rotational constants for five ^{13}C and deuterium isotopomers, obtained from published microwave spectra, were "corrected" into equilibrium rotational constants. The needed vibration−rotation interaction constants were computed with QC models after scaling the force constants. A semi-experimental equilibrium structure, fitted to the equilibrium moments of inertia, is $r_{C1C} = 1.470(1)$ Å, $r_{CC} = 1.546(1)$ Å, $r_{CF} = 1.343(1)$ Å, $r_{CH} = 1.078(1)$ Å, $\alpha_{FCF} = 109.5(1)$, $\alpha_{FCC} = 119.4(1)°$, $\alpha_{HCH} = 116.7(1)°$, $\alpha_{C1CH} = 117.4(1)°$, and $\alpha_{CCH} = 117.1(1)°$. This structure agrees within the indicated uncertainties with the ab initio structure obtained from an extrapolated set of CCSD(T)/aug-cc-pVnZ calculations except for $r_{CC} = 1.548$ Å. The F_2C-CH_2 bonds are significantly shortened and strengthened; the H_2C-CH_2 bond is significantly lengthened and weakened.

Introduction

Fluorine substitution for hydrogen exerts a potent effect on the CC bonds in small ring systems. CC bonds contiguous to a fluorine-substituted carbon atom are shortened; CC bonds distal to a fluorine-substituted carbon atom are lengthened. This effect is also reflected in force constants for CC stretching. Shortened bonds have larger force constants, and lengthened bonds have smaller force constants.

Table 1 shows the effect of fluorine substitution on CC bond lengths in cyclopropanes and cyclopropenes. Equilibrium structures are given in Table 1 for cyclopropane,[1] cyclopropene,[2] and 3,3-difluorocyclopropene.[2] The others are mostly substitution structures from microwave (MW) investigations. As an example of the effect of fluorine substitution, we consider 3,3-difluorocyclopropene in comparison with cyclopropene itself. In 3,3-difluorocyclopropene, the C−C bonds to the substituted carbon atom are shortened to 1.439 Å in comparison with a C−C bond length of 1.507 Å in cyclopropene.[2] The C═C bond in 3,3-difluorocyclopropene is lengthened to 1.319 Å in comparison with 1.294 Å in cyclopropene.[2] In Table 1, similar adjustments in CC bond lengths are seen in response to fluorine substitution in other C_3 rings.

Table 2 shows the effect of fluorine substitution on force constants for CC bonds in C_3 rings.[3] Table 2 is incomplete for cyclopropanes because, prior to this study, force constant information was known for only one molecule. In contrast, force constants for the whole suite of fluorocyclopropenes are available from a recent ab initio, scaled-force-constant study,[11] and experimental observations of fundamentals and empirical force constants are in the literature for all but two of these species.[12−16] Experimental values of fundamental frequencies are not known for 1-fluoro- and 1,2-difluorocyclopropene. The force constants from scaling, which are given in Table 2, are more reliable than the empirical force constants owing to the superior treatment of off-diagonal, interaction force constants. Although the vibrational spectra of three fluorocyclopropanes (1,1,2,2-, *cis*-, and *trans*-1,2-) and their deuterium isotopomers were studied in detail, empirical force constants were not fitted.[17,18]

To continue with the example selected from Table 1, we consider 3,3-difluorocyclopropene compared with cyclopropene. In 3,3-difluorocyclopropene, the force constant for a C−C bond to the substituted carbon atom has a value of 5.02 mdyn/Å, whereas the force constant is 3.84 mdyn/Å for the equivalent bond in cyclopropene.[11] The force constant for the C═C bond is 9.17 mdyn/Å in comparison with 10.11 mdyn/Å for the equivalent bond in cyclopropene.[11] As shown in Table 2, similar adjustments occur in other fluorocyclopropene species. Empirical force constant data for the cyclopropenyl cation and its various fluorine-substituted variants are also available.[19] However, these empirical force fields were fit with CC bond lengths that have been made suspect by the subsequent high-level ab initio calculations for $C_3H_3^+$ and $C_3F_3^+$ by Xie and Boggs.[20,21] Thus, we have not included the empirical force constants for $C_3H_3^+$, $C_3H_2F^+$, $C_3HF_2^+$, or $C_3F_3^+$ in Table 2 even though they follow the same pattern as for the other C_3 ring systems.

Although an MW investigation of several isotopomers of difluorocyclopropane (DFCP) led to a substitution structure for this species,[6] no vibrational spectroscopy has been reported. The present paper reports on the IR and Raman spectra of DFCP

* Corresponding author.
† Oberlin College.
‡ Washington State University.
§ University of Missouri−Kansas City.
|| University of Edinburgh

10.1021/jp0686947 CCC: $37.00 © 2007 American Chemical Society
Published on Web 03/10/2007

TABLE 1: Bond Lengths in C_3 Rings (in Å)

substance[a]	r_{C-C}	r_{FC-C}	r_{FC-CF}	r_{F_2C-C}	$r_{F_2C-CF_2}$	$r_{C=C}$	$r_{FC=CF}$
cyclopropane, r_e[b]	1.503(1)						
cis−1,2-difluorocyclopropane, r_s[c]		1.503(4)	1.488(3)				
trans−1,2-difluorocyclopropane, r_s[d]		1.488(5)	1.466(4)				
1,1-difluorocyclopropane, r_s[e]	1.553(1)			1.464(2)			
1,1,2,2-tetrafluorocyclopropane, r_s[f]				1.497(10)	1.471(3)		
perfluorocyclopropane, r_g[g]			1.505(3)				
cyclopropene, r_e[h]	1.507(1)					1.294(1)	
3,3-difluorocyclopropene, r_e[h]				1.439(1)		1.319(1)	
perfluorocyclopropene, r_e[i]				1.461(3)			1.307(13)

[a] Followed by type of structure: r_e, equilibrium; r_s, substitution; r_g, electron diffraction. [b] Reference 1; cf. new ab initio calculations in Equilibrium Structure. [c] Reference 4. [d] Reference 5. [e] Reference 6. [f] Reference 7. [g] Reference 8. [h] Reference 2; uncertainties 0.0004 or less. [i] Reference 9.

TABLE 2: Force Constants in C_3 Rings (in mdyn/Å)

substance	f_{C-C}	f_{FC-C}	f_{F_2C-C}	f_{F_2C-CF}	$f_{C=C}$	$f_{FC=C}$	$f_{FC=CF}$
cyclopropane[a]	3.99(5)						
cyclopropene[b,c]	3.84				10.11		
3-fluorocyclopropene[b,d]		4.54			9.58		
3,3-difluorocyclopropene[b,e]			5.02		9.17		
1,3,3-trifluorocyclopropene[b,f]			4.38	5.41		9.73	
perfluorocyclopropene[b,g]				4.79			10.08
1-fluorocyclopropene[b]	3.15	4.48				10.68	
1,2-difluorocyclopropene[b]		3.77					11.09

[a] Reference 10. [b] Reference 11. [c] Reference 12. [d] Reference 13. [e] Reference 14. [f] Reference 15. [g] Reference 16.

and its d_2 and d_4 isotopomers. Frequencies and intensities computed with quantum chemical (QC) calculations support the assignments of vibrational fundamentals. In a separate paper, a thorough normal coordinate analysis is reported. These calculations depend on adjusting scale factors for the QC harmonic force constants in symmetry coordinate space while fitting most of the observed fundamental frequencies of the three isotopomers. QC calculations of anharmonic $x_{i,j}$ terms with Gaussian 03[22] have aided the analysis of Fermi resonances and assignments of combination tones. Vibration−rotation constants are computed for the isotopomers and used to extract equilibrium rotational constants from ground state rotational constants. A culmination of this investigation is an equilibrium structure of DFCP, which is compared with optimized structures computed by QC methods.

Experimental Section

Syntheses. The isotopomers of DFCP were prepared by adding various methylene species to appropriate ethylenes. This chemistry and the separation by gas chromatography have been described in detail before.[23] DFCP itself was prepared by photolysis of a 1:5 mixture of ketene and 1,1-difluoroethylene (Matheson) in a Pyrex flask. The ketene was obtained from flash vacuum pyrolysis (FVP) of acetic anhydride in a quartz tube at 580 °C. DFCP-d_2 was prepared by photolysis of a mixture of ketene-d_2 and 1,1-difluoroethylene (Matheson) in the gas phase. Ketene-d_2 was obtained by FVP of acetone-d_6 at 725 °C. DFCP-d_4 was prepared by thermolysis of a mixture of perfluoropropylene oxide (PCR, Gainesville, FL) and ethylene-d_4 at 150 °C. MW spectra confirmed the identities of the d_0 and d_4 species.[6] The vibrational spectra and the similarity of the chemistry for making the d_2 species to the chemistry for making the d_0 species confirmed the identity of the d_2 species. The boiling point of DFCP was estimated as −6 °C from extrapolating observed vapor pressures according to the Clausius−Clapeyron equation. The melting point is −119 °C, as measured by a micro-method.

Spectroscopy. IR spectra were recorded as 300 scans on a Nicolet 760 Magna spectrometer in the gas phase in a 10 cm cell equipped with 2.5 cm diameter potassium bromide windows. The resolution was nominally 0.125 cm^{-1} and approximately 0.08 cm^{-1} unapodized, as was chosen. Far-IR spectra were recorded with 400 scans on a Perkin-Elmer 1700X instrument in a 10 cm cell equipped with 2.5 cm cesium iodide windows. The resolution of the far-IR spectrometer was 1 cm^{-1}. Both spectrometers were purged with dry nitrogen.

Raman spectra were recorded with the Raman module associated with the Nicolet 760 instrument. Excitation was with a Nd:YVO_4 laser, optics were for 180° observation of the scattered light, and the detector was liquid-nitrogen-cooled germanium. Typical laser power was 0.65 W. Spectra shown in this paper for liquid samples, which were sealed in 1.8 mm capillaries, were recorded with a 4 cm^{-1} resolution and 2500 scans. However, spectra were also recorded at a 2 cm^{-1} resolution to check for possible overlapping bands. Polarization information came from Raman spectra recorded on a Beckman 700 instrument with 4 cm^{-1} resolution, 90° optics, and 200 mW of excitation by the 488.0 nm line of an argon−ion laser. These additional Raman spectra were recorded a number of years ago at the College of Wooster.

Raman spectra were also recorded for gas-phase samples with the Nicolet system. Samples were sealed in standard 5 mm NMR tubes. A small pool of liquid in the bottom of the tube gave a vapor pressure of approximately 4 atm at 35 °C in the sample compartment. The sample was held in the cylindrical, gold-plated holder without additional optics to enhance the Raman signal. With a laser power of approximately 1.3 W, 15 000 scans were accumulated in separate blocks of 1000 scans.

Calculations. For support of the vibrational assignments of the three isotopomers of DFCP, optimized geometry, frequencies, IR intensities, Raman activities, and Raman depolarization ratios (90° optics) were computed with the B3LYP/cc-pVTZ model[24−26] and Gaussian 03 software.[22] For the companion paper on the normal coordinate analysis, calculations were made with three other models at the triple-ζ level. Geometry optimizations from all four calculations are reported in the present paper.

The calculation of the semi-experimental equilibrium (r_e) structure for DFCP was done in the same manner as described

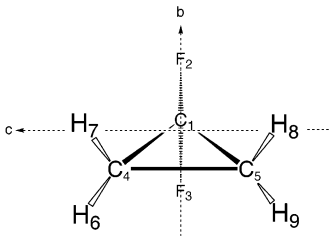

Figure 1. Schematic of 1,1-difluorocyclopropane. Principal rotation axes *b* and *c* are shown; the *a* rotation axis is also the twofold symmetry axis lying in the plane of the ring.

recently for butadiene and ethylene.[27] The ground state rotational constants were derived from the MW investigation of the d_0, d_0-2-$^{13}C_1$, d_4, d_4-1-$^{13}C_1$, and d_4-2-$^{13}C_1$ species.[6] The number of MW lines (a-type) was insufficient to fit a full set of quartic centrifugal distortion constants. The lines were refitted with full sets of quartic centrifugal distortion constants predicted with Gaussian 03 with the B3LYP/cc-pVTZ model.[22] The new *A*, *B*, and *C* rotational constants, which do not differ greatly from the rigid rotor ones, are reported in supplementary Table S1 (Supporting Information).

Vibration−rotation interaction constants (alphas) were computed from scaled QC force constants and other calculated molecular data and were used to convert ground state rotational constants into equilibrium rotational constants. Two methods for scaling the force constants were used.[27] In the more elaborate method, the harmonic force constants from the QC calculations were selectively scaled in symmetry coordinate space (diagonal values), whereas the cubic force constants remained unscaled. In the simpler method, a single average scale factor derived from the first method was applied to the harmonic force constants. For both methods, the cubic contributions to alphas came from the program VIBROT.[28] For the method with multiple scale factors for force constants, the harmonic contributions to alphas were from ASYM40.[29] For the method with the single scale factor, the harmonic contributions were from VIBROT.[28] The r_e structure came from a global fit to the set of equilibrium moments of inertia for the five isotopomers done with the program STRFIT.[30]

Results

Selection Rules. Figure 1 is a schematic of the structure of DFCP. For the d_0 and d_4 species, the C_2 axis of symmetry is also the *a* principal rotation axis and the direction of the dipole moment. The *c* rotation axis lies in the plane of the C_3 ring, and the *b* rotation axis is perpendicular to the C_3 ring. DFCP is a quite asymmetric top with $\kappa = -0.101$. As a consequence of the directions of the principal rotation axes for the d_0 and d_4 species, the seven modes of the a_1 symmetry species will have A-type band shapes in the gas-phase IR spectrum, the five modes of the b_1 symmetry species will have C-type band shapes, and the five modes of the b_2 symmetry species will have B-type band shapes. All modes are Raman active, and the modes of the a_2 symmetry species are inactive in the IR spectrum. For DFCP-d_2, the symmetry reduces to C_s with only the single plane of symmetry of the C_3 ring. The 12 modes of the a′ symmetry species correlate with the a_1 and b_1 symmetry species of the more symmetrical isotopomers, and 9 modes of the a″ symmetry species correlate with the a_2 and b_2 modes of the more symmetrical isotopomers. All modes for the d_2 species are IR and Raman active.

DFCP. Calculated and spectroscopic evidence in support of the assignments of the 21 vibrational fundamentals of DFCP is given in Table 3. The calculated values in Table 3 come from the B3LYP/cc-pVTZ model and are unscaled with the exception of the CH stretching frequencies, which were multiplied by 0.97. The selected values for the fundamentals, which are, with one exception, gas-phase values, are in the last column of the table. Figure 2 displays the mid-IR spectrum of the gas phase, and Figure 3 shows the far-IR spectrum of the gas phase. The Raman spectrum of the liquid phase without polarization analysis is in Figure 4. A gas-phase Raman spectrum, which has fewer bands, is supplied as supplementary Figure S1 (Supporting Information).

Most of the assignments of vibrational fundamentals for DFCP are well-supported by experimental data. For DFCP, the four CH stretching frequencies have the useful characteristic of each belonging to a different symmetry species. In addition, these upper states of the fundamental bands concerned appear to be essentially free of Fermi resonance, an outcome which is highly unusual for CH stretching transitions. The correlation between predicted and observed IR intensities and Raman activities is good. These predictions are especially helpful in making assignments in the crowded spectral region from 930 to 1100 cm^{-1} and in reinforcing the interpretation of three instances of Fermi resonance for ν_2, ν_6, and ν_{14}. One of these resonances, ν_{14}, lies in the crowded region. Assignments of Fermi resonances are reinforced by the resonances reappearing in higher frequency combinations. In most cases the band shapes in the gas-phase IR spectrum and depolarization ratios in the Raman spectra support the assignments. Table S2 (Supporting Information) includes the assignments of combination and difference transitions. These assignments are reinforced by the use of anharmonic $x_{i,j}$ constants computed with Gaussian 03 and the B3LYP/6-311++G** model.[22]

Only for some of the a_2 modes, which are only Raman active, is experimental support incomplete. The assignment for ν_9, which has a weak feature in the liquid-phase Raman spectrum at 1151 cm^{-1}, is based on a Q branch at 1153 cm^{-1} in the IR spectrum, presumed to have been made active by a Coriolis perturbation. No direct experimental data exist for ν_{10}, which is predicted to have a Raman activity of only 0.02 Å^4/amu. The value of 879 cm^{-1} given for this mode comes from the detailed normal coordinate calculations reported in a separate paper. The gas-phase value of 335 cm^{-1} for ν_{11} is estimated from combination tones, which are supplied in Table S2. This value is also consistent with the liquid-phase value from the Raman spectrum and the MW determination of approximately 327 cm^{-1}, as deduced from the temperature dependence of intensities for rotational transitions in the ground state and excited vibrational state.[6] The ν_{21} mode of the b_2 symmetry species is predicted to have an IR intensity of only 0.60 km/mol and is seen weakly in the far-IR spectrum with a probable B-type band shape. However, there can be no doubt about this assignment because of supporting combination tones and the confirming value of 351 cm^{-1} deduced from observations in the MW region.[6]

As is shown in the normal coordinate paper, all of the fundamental frequencies for DFCP are predicted with four QC models and scaled force constants within 6 cm^{-1} with three exceptions. Thus, we have high confidence in these assignments. Details of all of the spectra and the assignments are in Table S2. Omitted from Table S2 are numerous Q-branch features in the vicinity of fundamentals, which are regarded as hot band transitions.

DFCP-d_4. As for the normal species, strong spectral evidence exists for all of the fundamentals except those of the a_2

TABLE 3: Computational and Spectroscopic Evidence for the Vibrational Fundamentals of 1,1-Difluorocyclopropane (in cm^{-1})

			predictions (B3LYP/cc-pVTZ)				observations					
			IR		Raman		IR		Raman frequency			
symmetry	mode	frequency[a]	I[b]	sh[c]	A[d]	dpol[e]	frequency	I[f],shape[c]	gas	liquid	A[f,g], dpol[e]	selected frequency
a_1	ν_1	3048	0.002	A	200	0.05	3037	w, Q	3038	3031	s, pol	3038
	ν_2	1515	107	A	2.7	0.21	1488[h]	s, A	1476	1471	wm, pol	1488[h]
	ν_3	1370	110	A	12	0.18	1351	s, A	1352	1347	m, pol	1351
	ν_4	1033	28	A	1.5	0.12	1007	sm, A		1009	w, pol	1007
	ν_5	967	21	A	19	0.08	952	sm, A?	953	947	vs, pol	952
	ν_6	711	11	A	6.5	0.67	702[h]	m, A?	701	701	m, pol	702[h]
	ν_7	467	9.0	A	1.7	0.70	468	m, A		472	m, pol	468
a_2	ν_8	3130			87	0.75			3114	3112	m, dp	3114
	ν_9	1181			2.9	0.75	1153	w, Q		1151	w, dp	1153
	ν_{10}	892			0.02	0.75						879[i]
	ν_{11}	333			0.99	0.75				340	m, dp	335[j]
b_1	ν_{12}	3047	5.0	C	20	0.75	3035	w, C		3031[k]		3035
	ν_{13}	1446	4.4	C	6.1	0.75	1409	w, C		1408	w, dp	1409
	ν_{14}	1095	17	C	2.7	0.75	1075[h]	m, C				1075[h]
	ν_{15}	1048	56	C	2.8	0.75	1032	s, C		1039	w, dp	1032
	ν_{16}	534	2.6	C	2.9	0.75	534	w, C		534	m, dp	534
b_2	ν_{17}	3141	2.5	B	23	0.75	3120	w, B	3114[l]	3112[l]	m, dp	3120
	ν_{18}	1284	131	B	0.002	0.75	1283	vs, B				1283
	ν_{19}	937	57	B	5.5	0.75	935	sm, B	934?	934	m, dp?	935
	ν_{20}	760	0.96	B	0.68	0.75	750	w, B		746	w, dp?	750
	ν_{21}	350	0.60	B	0.003	0.75	350	vw, B				350[m]

[a] Four CH stretching frequencies scaled by 0.97; other frequencies unscaled. [b] IR intensity in km/mol. [c] Band shape in gas-phase IR. [d] Raman activity in Å^4/amu. [e] Depolarization ratio for 90° optics. [f] v, very; s, strong; m, medium; w, weak. [g] For liquid phase. [h] Adjusted for Fermi resonance. [i] From calculation with scaled B3LYP/cc-pVTZ force constants. [j] Estimated from combination tones; consistent with MW observation of approximately 327 cm^{-1} in ref 6. [k] Overlap with ν_1. [l] Overlap with ν_8. [m] Consistent with the MW observation of approximately 351 cm^{-1} in ref 5.

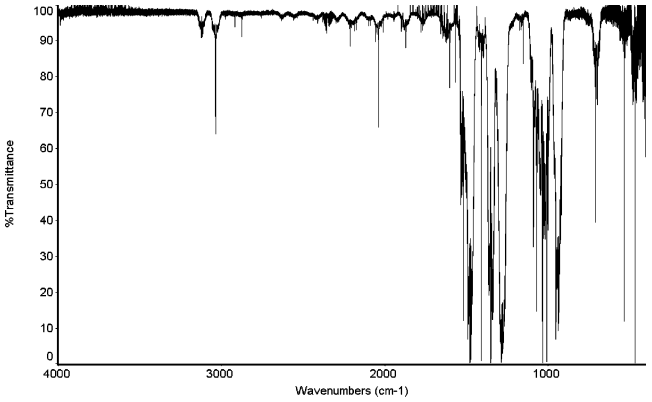

Figure 2. Mid-IR spectrum of 1,1-difluorocyclopropane in the gas phase at 15 Torr pressure.

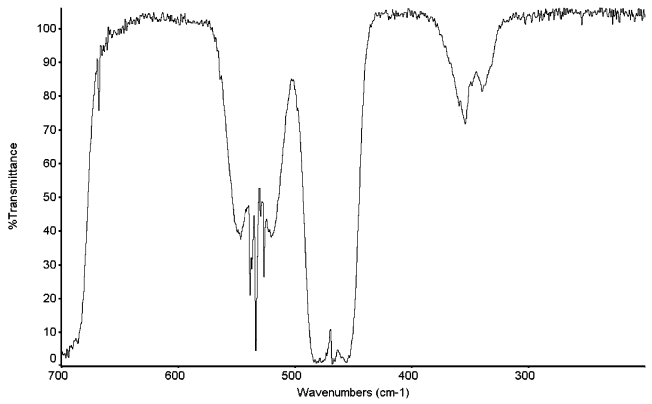

Figure 3. Far-IR spectrum of 1,1-difluorocyclopropane in the gas phase at 384 Torr pressure.

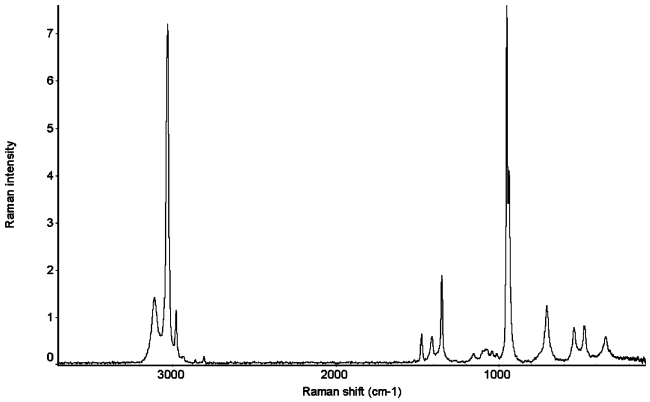

Figure 4. Raman spectrum of 1,1-difluorocyclopropane in the liquid phase without a polarization analyzer.

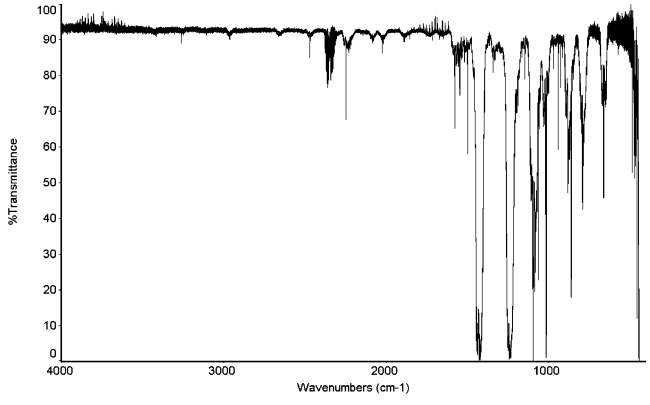

Figure 5. Mid-IR spectrum of 1,1-difluorocyclopropane-d_4 in the gas phase at 15 Torr pressure.

symmetry species, which are only Raman active. Gas-phase IR spectra are in Figures 5 and 6. Although the far-IR spectrum in Figure 6 is too intense to show the shape for the band at 454 cm^{-1}, an A-type band shape was evident in other scans for this species. The liquid-phase Raman spectrum is in Figure 7, and the gas-phase Raman spectrum is available as Figure S2

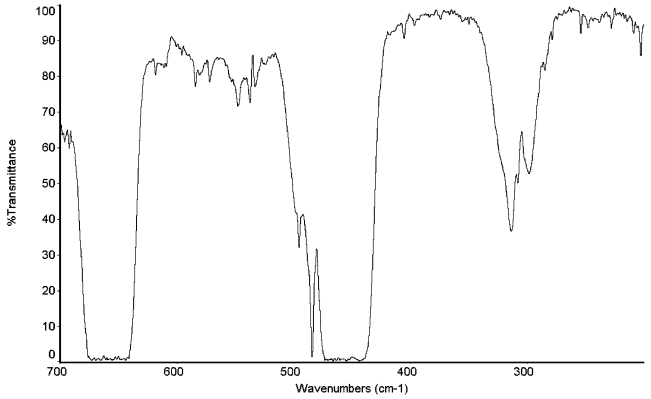

Figure 6. Far-IR spectrum of 1,1-difluorocyclopropane-d_4 in the gas phase at 565 Torr pressure.

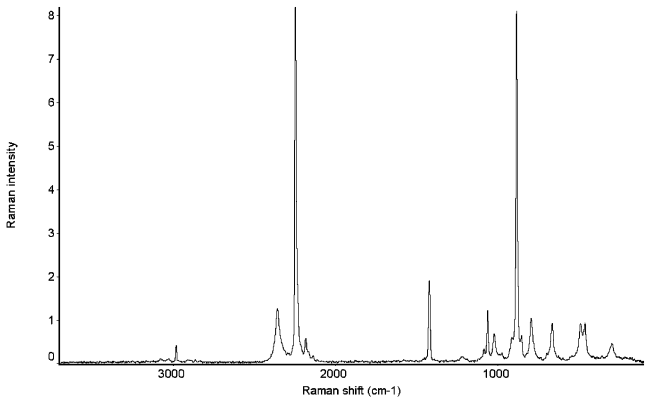

Figure 7. Raman spectrum of 1,1-difluorocyclopropane-d_4 in the liquid phase without a polarization analyzer.

(Supporting Information). The evidence for the assignments of fundamentals is summarized in Table 4. The last column of Table 4 gives the selected frequencies for the fundamentals. Assignments in the crowded region from 1000 to 1220 cm^{-1}, including Fermi resonances for ν_3 and ν_{13}, are supported by the frequency and intensity predictions.

We focus this discussion on the a_2 modes, which contain the more doubtful assignments. Good evidence for ν_8 in the CH stretching region at 2351 cm^{-1} comes from the gas-phase and the liquid-phase Raman spectra. As for the d_0 species, a weak Q branch at 911 cm^{-1} in the gas-phase IR spectrum, which is attributed to a Coriolis interaction, is assigned to ν_9. This assignment is supported by a weak band of uncertain polarization in the liquid-phase Raman spectrum at 909 cm^{-1}. For ν_{10}, for which the predicted Raman activity is a mere 0.006 $Å^2$/amu, no direct spectral evidence exists. The assignment of ν_{10} at 653 cm^{-1} is derived from combination tones, which are reported in Table S3 (Supporting Information), and is supported by agreement within 2 cm^{-1} in force constant scaling. For ν_{11}, a weak depolarized feature is at 292 cm^{-1} in the liquid-phase Raman spectrum. The selected frequency of 287 cm^{-1} for this mode comes from assignments of combination tones in the gas-phase spectrum. One other assignment deserves mention. For ν_{21} (b_2), the spectral evidence is a distorted B-type band in the gas-phase IR spectrum with an approximate band center of 308 cm^{-1}. On the basis of combination tones, a value of 310 cm^{-1} is selected for this frequency.

Table S3 reports the details of all of the spectra and of the assignments, which are satisfactory with rare exception. Apart from low values for CD_2 stretching modes due to scaling the CH stretching force constant to CH_2 stretching frequencies and from the differing effects of anharmonicity for CH and CD stretching, the largest error in any of the four models was 8.0 cm^{-1} for ν_{14}. All considered, the evidence is compelling for the assignments of all of the vibrational fundamentals of DFCP-d_4.

DFCP-d_2. The lower C_s symmetry for the d_2 species makes all of the modes IR active as well as Raman active and produces direct spectral evidence for all of the 21 fundamentals. The

TABLE 4: Computational and Spectroscopic Evidence for the Vibrational Fundamentals of 1,1-Difluorocyclopropane-d_4 (in cm^{-1})

		predictions (B3LYP/cc-pVTZ)					observations					
			IR		Raman		IR		Raman frequency		Raman	selected
symmetry	mode	frequency	I^a	sh[b]	A^c	dpol[d]	frequency	I^e, shape[b]	gas	liquid	$A^{e,f}$, dpol[d]	frequency
a_1	ν_1	2288	1.6	A	89	0.06	2247	w, A	2247	2243	s, pol	2247
	ν_2	1436	201	A	11	0.01	1428	vs, A	1427	1417	m, pol	1428
	ν_3	1091	25	A	2.1	0.13	1066[g]	m, A?	1063	1058	wm, pol	1066[g]
	ν_4	899	15	A	20	0.14	879	m, A	881	879	vs, pol	879
	ν_5	811	0.03	A	2.1	0.21	794	w, Q	795	789	wm, pol	794
	ν_6	662	12	A	4	0.71	658	m, A		661	wm, pol	658
	ν_7	454	11	A	1.8	0.68	454	m, A	454	459	wm, pol	454
a_2	ν_8	2411			43	0.75			2351	2355	wm, dp	2351
	ν_9	924			3.0	0.75	911	vw, Q		909	w, dp?	911
	ν_{10}	671			0.006	0.75						653[h]
	ν_{11}	286			0.64	0.75				292	w, dp	287[i]
b_1	ν_{12}	2275	0.72	C	8.8	0.75	2228	w, Q		2233	m, ?	2228
	ν_{13}	1102	43	C	0.23	0.75	1091[g]	s, C		1094	w, dp?	1091[g]
	ν_{14}	1022	25	C	7.0	0.75	1013	m, C		1017	wm, dp	1013
	ν_{15}	877	7.8	C	0.13	0.75	858	m, C				858
	ν_{16}	484	1.9	C	2.6	0.75	484	w, C		485	wm, dp	484
b_2	ν_{17}	2412	1.4	B	11	0.75	2353	w, B	2351[j]	2355	m, dp	2353
	ν_{18}	1229	168	B	0.50	0.75	1239	vs, B		1218	w, dp	1239
	ν_{19}	788	20	B	3.9	0.75	787	m, B	795[k]	789	wm, dp?	787
	ν_{20}	543	0.22	B	0.30	0.75	538	vw, B?		539	vw, dp?	538
	ν_{21}	310	0.95	B	0.003	0.75	308	w, B				310[i]

[a] IR intensity in km/mol. [b] Band shape in gas-phase IR. [c] Raman activity in $Å^4$/amu. [d] Depolarization ratio for 90° optics. [e] v, very; s, strong; m, medium; w, weak. [f] For liquid phase. [g] Adjusted for Fermi resonance. [h] From calculation with scaled B3LYP/cc-pVTZ force constants. [i] Estimated from combination tones. [j] Overlap with ν_8. [k] Overlap with ν_5.

TABLE 5: Computational and Spectroscopic Evidence for the Vibrational Fundamentals of 1,1-Difluorocyclopropane-d_2 (in cm^{-1})

		predictions (B3LYP/cc-pVTZ)					observations					
			IR		Raman		IR		Raman frequency			
symmetry	mode	frequency[a]	I[b]	sh[c]	A[d]	dpol[e]	frequency	I[f], shape[c]	gas	liquid	A[f,g], dpol[e]	selected frequency
a′	ν_1	3047	2.5	A/C	110	0.09	3035	w, C	3036	3031	s, pol	3035
	ν_2	2281	1.2	A/C	48	0.10	2236	w, C	2235	2232	s, pol	2236
	ν_3	1493	99	A/C	4.6	0.24	1468	s, A	1469	1464	m, pol	1468
	ν_4	1391	111	A/C	11	0.17	1370	s, A/C		1368	sm, pol	1370
	ν_5	1100	40	A/C	1.2	0.38	1088	m, A		1092	w, pol	1088
	ν_6	1067	2.7	A/C	2.7	0.63	1047[h]	w, Q		1047	wm, pol	1047
	ν_7	1038	54	A/C	4.7	0.39	1019[h]	m, A		1020	m, pol	1019
	ν_8	927	19	A/C	19	0.12	906	sm, C?	906	903	vs, pol	906
	ν_9	838	2.4	A/C	1.1	0.25	820	w, C		821	w, pol	820
	ν_{10}	692	12	A/C	5.5	0.69	687	wm,A/C		688	m, pol	687
	ν_{11}	509	2.2	A/C	2.6	0.749	509	w, A/C		511	m, pol	509
	ν_{12}	458	9.7	A/C	1.8	0.69	459	wm, A		462	m, pol	459
a″	ν_{13}	3136	1.2	B	55	0.75	3115	w, B	3119	3114	w, dp	3115
	ν_{14}	2412	0.68	B	27	0.75	2357	w, B	2351	2355	w, dp	2357
	ν_{15}	1258	145	B	0.15	0.75	1262	vs, B		1241	vw, dp?	1262
	ν_{16}	1077	4.1	B	3.2	0.75				1061	m, dp?	1061[i]
	ν_{17}	922	35	B	3.7	0.75	917	s, B		919	m, ?	917
	ν_{18}	726	3.6	B	0.89	0.75	720	w, B		720	w, dp	720
	ν_{19}	628	0.60	B	0.72	0.75	620	vw, B		621	vw, dp	620
	ν_{20}	332	0.65	B	0.12	0.75	332	vw, B		333	w, dp	332
	ν_{21}	302	0.15	B	0.64	0.75	301	vw, B		308	wm, dp	301

[a] Two CH stretching frequencies scaled by 0.97; other frequencies unscaled. [b] IR intensity in km/mol. [c] Band shape in gas-phase IR. [d] Raman activity in Å^4/amu. [e] Depolarization ratio for 90° optics. [f] v, very; s, strong; m, medium; w, weak. [g] For the liquid phase. [h] Adjusted for Fermi resonance. [i] From the liquid phase.

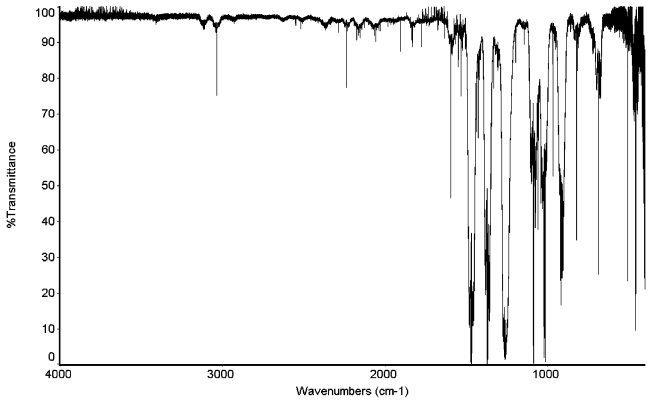

Figure 8. Mid-IR spectrum of 1,1-difluorocyclopropane-d_2 in the gas phase at 15 Torr pressure.

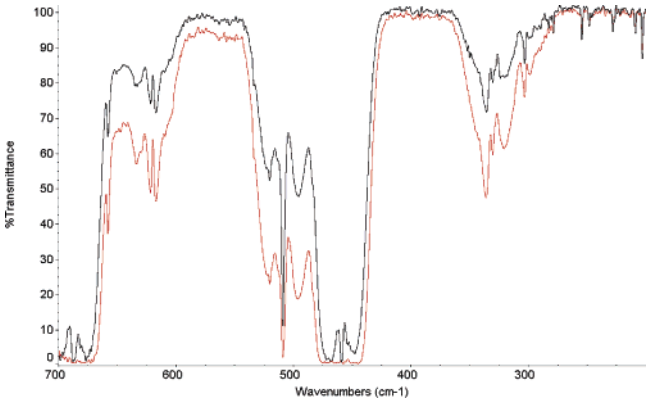

Figure 9. Far-IR spectrum of 1,1-difluorocyclopropane-d_2 in the gas phase at 272 and 544 Torr pressure.

observations and calculations that support these assignments are presented in Table 5. Figures 8 and 9 display the gas-phase IR spectra. Figure 10 is the Raman spectrum for the liquid phase without polarization analysis. Table S4 (Supporting Information) provides details of all the assignments, including weak features assigned to combination and difference bands. As for the assignments for the other two isotopomers, the frequency and intensity predictions are especially helpful in the crowded region of 1000−1100 cm^{-1}, which contains the two instances of Fermi resonance.

Direct spectral evidence for all but one of the vibrational fundamentals of the d_2 species is found in the gas-phase IR spectrum. In most cases, the band shapes are definitive. Where the band shapes are not definitive, polarization ratios from the Raman spectrum provide convincing evidence. For only one mode is a gas-phase frequency unavailable. For ν_{16}, the liquid-phase Raman frequency is adopted. Although the intensity predicted of 4.1 km/mol for the IR transition should be observable, the crowding of bands in this region causes doubt. In the gas-phase IR spectrum in Figure 5, the band for CD_2 stretching at 2353 cm^{-1} appears to be overshadowed by the carbon dioxide impurity band in this region. However, in the detailed spectrum, the contour of a B-type band is clearly seen.

Table S4 gives the details of the spectra and of the assignments for all of the combination tones. Frequencies calculated with scaled force constants agree with observed fundamental frequencies within 7 cm^{-1}. Frequencies for ν_1 and ν_{13} for CH_2 stretching were fit exactly in the scaling exercise.

Equilibrium Structure. The equilibrium structure of DFCP has been determined by the "semi-experimental" method, which was recently described in full as applied to ethylene and butadiene.[27] In this method, vibration−rotation constants, also known as spectroscopic alphas, were calculated from force constants, optimized geometries, and frequencies from calculations with several QC models, as described in Calculations.[22,28,29] With use of the vibration−rotation constants, the observed ground state rotational constants were "corrected" to equilibrium rotational constants, which were transformed into moments of

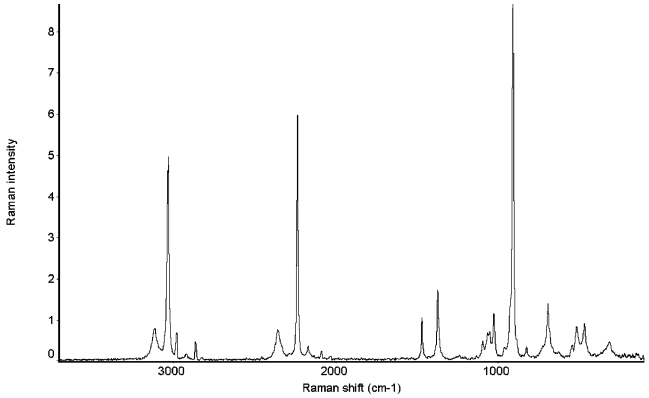

Figure 10. Raman spectrum of 1,1-difluorocyclopropane-d_2 in the liquid phase without a polarization analyzer.

inertia for structure fitting. Table 6 compares the ground state moments of inertia for the five available isotopomers of DFCP with one set of equilibrium moments of inertia. The equilibrium moments of inertia in Table 6 were derived from the selectively scaled force constants for the B3LYP/cc-pVTZ model. In general, the equilibrium moments of inertia are smaller than the ground state moments of inertia because the molecule is more compact in the absence of vibrations in the equilibrium form. One indicator of the success in obtaining equilibrium moments of inertia is a comparison of the I_{ea} equilibrium moments of inertia for the d_4 and d_4-1-$^{13}C_1$ species. These values should be the same because the 1-^{13}C atom lies on the *a* rotational axis. These two values differ by only 0.000 11%. Table S5 (Supporting Information) is an example of computing the equilibrium rotational constants by the two methods from the ground state rotational constants and the calculated vibration−rotation constants. Table S5, which is for the B3LYP/cc-pVTZ model, shows the relative harmonic and cubic contributions to the vibration−rotation constants for the five isotopomers.

Table 7 gives the detailed results of structure fitting to the equilibrium moments of inertia obtained with alpha contributions from the four QC models at the triple-ζ level. Two of these models were based on density functional theory (DFT): B3LYP/cc-pVTZ and B3LYP/6-311++G**. The other two rely on the second-order Møller−Plesset perturbation theory (MP2): MP2/cc-pVTZ and MP2/6-311++G**. Bond lengths and bond angles derived from the alphas from four models with selective scaling of the force constants are listed in Table 7. The second-to-last column gives the averages of the bond parameters from the four models. The last column in Table 7 contains the corresponding averages of bond parameters obtained with the simpler, single-scale-factor method. The differences between the average results for the two approaches are negligible. Thus, the simpler method with the single average scale factor for force constants suffices at the triple-ζ basis set level. We regard the uncertainty in the estimates to be 0.001 Å or 0.1°; these values span the range of values obtained with the different models.

The stability of the solution of the structure of DFCP obtained from equilibrium moments of inertia is remarkable because of the small *a* coordinate (−0.086 Å) for C_1. It is well-known that small coordinates compromise structure determinations in the traditional methods used by MW spectroscopists.[6]

We turn to comparisons of various calculated structures and one experimental structure with the semi-experimental equilibrium structure of DFCP. Table 8 includes the bond parameters of the optimized structures computed with the four QC models used to compute the vibration−rotation constants. After the semi-experimental structure had been found, two other ab initio calculations were done at a higher level of theory. One of these calculations was with the MP2/cc-pVQZ model. These results are in column five of numerical data in Table 8. The ultimate calculation was at a higher level of theory, in which optimized internal coordinates were computed with MOLPRO 2006[31] at the frozen core CCSD(T)/aug-cc-pVnZ, n = D, T and Q, levels of theory. Estimated complete basis set structural parameters were then obtained by extrapolating the bond lengths and angles with a simple exponential functional form.[32] Small core/valence and scalar relativistic corrections, obtained from CCSD(T)/cc-pCVQZ and CCSD(T)-DK/cc-pVTZ_DK calculations, were included. (This method was also applied to cyclopropane.[33]) The results of the CCSD(T) calculations for DFCP are in the third-from-last column in Table 8. The next-to-last column in this table contains the bond parameters in the r_s substitution structure reported from the MW investigation by Perretta and Laurie.[6] As has been seen before in comparing substitution structures with equilibrium structures, the substitution structure of DFCP is uncertain in the ranges of ±0.01 Å and ±1°. An equilibrium structure is needed for an accuracy of 0.001 Å in making comparisons with other structures.

In Table 8, the bond parameters from optimized structures that agree with the r_e structure within 0.002 Å or 0.2° are shown in boldface type. The agreement between the semi-experimental equilibrium structure and the high-level CCSD(T) structure is outstanding. The favorable comparison is noteworthy because DFCP is only the second example of an application to a molecule with fluorine substitution and alphas computed with triple-ζ QC theory. In addition, the absence of fluorine isotopomers could compromise the semi-experimental structure, and the presence of fluorine atoms challenges the ab initio calculations. The agreement between the semi-experimental structure and the ab initio structure reinforces our belief that semi-experimental structures for small molecules are now reliable to ∼0.001 Å. On the basis of extensive benchmarking, the CCSD(T) bond lengths reported here are expected to have an uncertainty of 0.001−0.002 Å.[34] The primary deficiency in the present calculations is the neglect of higher order electron correlation effects.

For the triple-ζ basis set models, the agreement is best for the MP2/cc-pVTZ model and almost as good for the B3LYP/cc-pVTZ model. The principal weakness in the B3LYP/cc-pVTZ

TABLE 6: Ground State and Equilibrium Moments of Inertia for 1,1-Difluorocyclopropane and Isotopomers (in AMU Å^2)

	ground state[a]			equilibrium[b]		
molecule	I_{0a}	I_{0b}	I_{0c}	I_{ea}	I_{eb}	I_{ec}
DFCP	70.3538(2)	90.8165(1)	119.0988(1)	69.8574	90.0281	118.2900
DFCP-2-$^{13}C_1$	70.9368(15)	92.7649(2)	120.4650(4)	70.4337	91.9641	119.6492
DFCP-d_4	80.2646(8)	105.3029(1)	130.5256(2)	79.6847	104.4327	129.6474
DFCP-d_4-1-$^{13}C_1$	80.2580(4)	105.3151(1)	130.5328(1)	79.6856	104.4571	129.6732
DFCP-d_4-2-$^{13}C_1$	80.8480(14)	107.0911(2)	131.7302(3)	80.2652	106.2121	130.8464

[a] Reference 6 and refitting with quartic centrifugal distortion constants from predictions with the B3LYP/cc-pVTZ model. [b] Computed with vibration−rotation constants from B3LYP/cc-pVTZ results and selective scaling of force constants.

TABLE 7: Equilibrium Structural Parameters for 1,1-Difluorocyclopropane

	calculated with QC models				semi-experimental	
parameter	B3LYP/ cc-pVTZ	B3LYP/ 6-311++G**	MP2/ cc-pVTZ	MP2/6-311++G**	r_e selected scale factors[a]	r_e single scale factor[b]
r(C−F)	1.3432	1.3437	1.3423	1.3418	**1.3428(10)**	1.3427
r(C−H)	1.0774	1.0775	1.0780	1.0777	**1.0777(10)**	1.0776
$r(C_1-C_4)$	1.4699	1.4695	1.4702	1.4709	**1.4701(10)**	1.4702
$r(C_4-C_5)$	1.5466	1.5468	1.5452	1.5450	**1.5459(10)**	1.5460
α(FCF)	109.41	109.34	109.51	109.58	**109.46(10)**	109.46
α(FCC)	119.43	119.45	119.40	119.38	**119.42(10)**	119.42
$\alpha(C_4C_1C_5)$	63.48	63.52	63.40	63.36	**63.44(10)**	63.44
$\alpha(C_1C_4C_5)$	58.26	58.24	58.30	58.32	**58.28(10)**	58.28
α(HCH)	116.79	116.80	116.65	116.68	**116.73(10)**	116.74
$\alpha(HC_4C_1)$	117.36	117.34	117.40	117.37	**117.37(10)**	117.37
$\alpha(HC_4C_5)$	117.13	117.13	117.20	117.19	**117.14(10)**	117.14
SD × 10^4 [c]	5.1	4.8	5.2	6.6		

[a] Average from using selected scale factors for harmonic force constants. [b] Based on single scale factor for harmonic force constants: B3LYP/cc-pVTZ, 0.9706; B3LYP/6-311++G**, 0.9812; MP2/cc-pVTZ, 0.9409; and MP2/6-311++G**, 0.9373. [c] Standard deviation × 10^4 in fitting to moments of inertia.

TABLE 8: Comparison of Calculated and Observed Geometric Parameters for 1,1-Difluorocyclopropane

	calculated with QC models[a]						observed	
parameter	B3LYP/ cc-pVTZ	B3LYP/ 6-311++G**	MP2/ cc-pVTZ	MP2/6-311++G**	MP2/aug-cc-pVQZ	CCSD(T)[b]	substitution r_s	equilibrium r_e
r(C−F)	1.3530	1.3590	**1.3454**	1.3517	1.3462	**1.3437**	1.355(2)	**1.343(1)**
r(C−H)	**1.0802**	1.0827	**1.0780**	1.0831	**1.0774**	**1.0786**	1.082(2)	**1.078(1)**
$r(C_1-C_4)$	**1.4723**	1.4742	**1.4707**	1.4740	**1.4687**	**1.4693**	1.464(2)	**1.470(1)**
$r(C_4-C_5)$	**1.5472**	1.5522	1.5493	1.5565	**1.5471**	**1.5485**	1.553(1)	**1.546(1)**
α(FCF)	109.21	109.00	**109.65**	**109.59**	**109.46**	**109.4**	108.3(2)	**109.5(1)**
α(FCC)	**119.53**	**119.58**	**119.32**	**119.31**	**119.39**	**119.4**		**119.4(1)**
$\alpha(C_4C_1C_5)$	**63.40**	**63.53**	**63.57**	63.74	**63.61**	**63.6**	64.1(1)	**63.4(1)**
$\alpha(C_1C_4C_5)$	**58.30**	**58.23**	**58.22**	**58.13**	**58.19**	**58.2**		**58.3(1)**
α(HCH)	116.00	116.02	**116.89**	**116.92**	116.95	**116.6**	116.9(2)	**116.7(1)**
$\alpha(HC_4C_1)$	117.67	**117.64**	**117.45**	**117.47**	**117.37**	**117.4**		**117.4(1)**
$\alpha(HC_4C_5)$	117.47	117.50	**116.96**	**116.94**	**116.95**	**117.2**		**117.1(1)**

[a] Boldface values (rounded) are within ±0.002 Å or 0.2° of the r_e values. [b] Frozen core CCSD(T)/aug-cc-pVnZ, n = D, T, and Q with extrapolations and corrections (see text).

model is the overestimation of the CF bond length. The HCH bond angle is also too small. Similarly, favorable agreement between triple-ζ QC models and the r_e structure was found for butadiene.[27] As expected, the agreement with the MP2/cc-pVQZ model is better than that for the triple-ζ models.

Comparison of the semi-experimental equilibrium CC bond length of cyclopropane (Table 1) and DFCP confirms the strong influence of fluorine substitution on the bond lengths in this C_3 ring system. The C−C bond to the fluorine-substituted carbon decreases in length by 0.033 Å, and the distal C−C bond increases in length by 0.043 Å. Thus, this interesting effect of fluorine substitution seen in the r_s structure is reinforced by the r_e structure.

From our normal coordinate calculations with scaled force constants, the force constant for the CC bonds to the fluorine-substituted carbon atom in DFCP is 4.69(6) mdyn/Å in comparison with 3.99 mdyn/Å for cyclopropane.[10] The force constant for the distal CC bond in DFCP is 3.40(6) mdyn/Å. (The uncertainties in these force constants for DFCP span the range of values found through scaling the force constants from the four triple-ζ QC models.) Thus, we find that the general strengthening−weakening effect of fluorine substitution in C_3 ring systems is present in force constants as well as in bond lengths in DFCP.

A full comparison between the equilibrium structures of cyclopropane and DFCP yields some secondary effects of fluorine substitution in the C_3 ring system, which can only be seen with the accuracy of equilibrium structures. For cyclopropane, the equilibrium C−H bond length is 1.0786(10) Å, and the equilibrium H−C−H bond angle is 114.97(10).[1] Thus, in DFCP, the C−H bond shortens by 0.0009 Å, and the H−C−H bond angle increases by 1.76° in comparison with cyclopropane. Compared with cyclopropane, the lengthening of one C−C bond to the hydrogen-bearing carbon atoms is greater than the shortening of the other type of C−C bond. The longer C−C bond should have increased p orbital character, and thus the C−H bond should have more s orbital character, which would make the CH bond shorter, as is observed. However, the decrease in the CCH bond angle in going to DFCP reflects an opposite effect, that is, increased p orbital character in the C−H bond in DFCP.

Conclusions

From IR and Raman spectra of DFCP and its d_2 and d_4 isotopomers and from QC calculations of frequencies and intensities, a complete assignment of the vibrational fundamentals has been derived. In a separate paper, detailed normal coordinate analysis gives strong support to these assignments, which include several Fermi resonance deperturbations for each isotopomer. Using vibration−rotation constants derived from scaled force constants obtained from four QC models at the triple-ζ basis set level to "correct" ground state rotational constants leads to concordant results for the equilibrium structure of DFCP. The equilibrium structure obtained with the simpler procedure of a single, average scale factor for the force constants is comparable to the structure obtained with multiple scale factors for the force constants. An extrapolated ab initio calculation of bond parameters with CCSD(T) theory gives an

equilibrium structure in excellent agreement with the semi-experimental structure. At the triple-ζ basis set level of theory, the optimized geometry for DFCP from the MP2/cc-pVTZ model agrees best with the equilibrium structure, and the DFT-based B3LYP/cc-pVTZ structure is a close second. An optimized structure computed with the MP2/cc-pVQZ theory is almost as good as the extrapolated CCSD(T) structure. The substantial changes in CC bond lengths found previously for DFCP with an r_s substitution structure are confirmed by the equilibrium structure. The CC bonds to the fluorine-substituted carbon atom are shortened by 0.033 Å, and the distal CC bond is lengthened by 0.043 Å in comparison with the equilibrium structure of cyclopropane. The force constant for the F_2C-CH_2 bond is appreciably greater than the CC force constant in cyclopropane, and the force constant for the H_2C-CH_2 bond in DFCP is smaller. Thus, both bond length and force constant adjustments in DFCP reflect a potent influence of fluorine substitution.

Acknowledgment. We are grateful to former Oberlin students, Peter H. Martyn, Amy A. Schaub, David A. Spiegel, Jeffrey B. Byer, and Peter J. Acker, who participated in the preliminary stages of this investigation. We thank Professors Richard Bromund and David Powell at the College of Wooster for providing access to the Beckman 700 Raman spectrometer. The research was supported by a grant from the Camille and Henry Dreyfus Foundation and by Oberlin College.

Supporting Information Available: Revised fitting of the rotational constants for the five isotopomers of DFCP (Table S1); details of the observations and assignments of observed frequencies for DFCP (Table S2); details of the observations and assignments of observed frequencies for DFCP-d_4 (Table S3); details of the observations and assignments of observed frequencies for DFCP-d_2 (Table S4); sample calculation of equilibrium rotational constants from ground state rotational constants and B3LYP/cc-pVTZ alphas (Table S5); gas-phase Raman spectrum of DFCP (Figure S1); gas-phase Raman spectrum of DFCP-d_4 (Figure S2); gas-phase Raman spectrum of DFCP-d_2 (Figure S3). This material is available free of charge via the Internet at http://pubs.acs.org.

References and Notes

(1) Gauss, J.; Cremer, D.; Stanton, J. F. *J. Phys. Chem. A* **2000**, *104*, 1319−1324.

(2) Krasnoshchekov, S. V.; Stepanov, N. F. *Russ. J. Phys. Chem.* **2006**, *80*, 1448−1455.

(3) The three stretching coordinates for the CC bonds provide a kinematically complete description of the ring stretching. This description for C_3 rings has been widely used in the literature. However, some angle bending is involved along with bond stretching in the symmetry coordinates for C_4-C_5 stretching (a_1) and for antisymmetric $C_4-C_1-C_5$ stretching (b_1). Some angle bending contributes to the CC force constants presented in Table 2, although this contribution is small because of the inherently smaller force constants for angle bending.

(4) Justnes, H.; Zozom, J.; Gillies, C. W.; Sengupta, S. K.; Craig, N. C. *J. Am. Chem. Soc.* **1986**, *108*, 881−887.

(5) Sengupta, S. K.; Justnes, H.; Gillies, C. W.; Craig, N. C. *J. Am. Chem. Soc.* **1986**, *108*, 876−880.

(6) Perretta, A. T.; Laurie, V. W. *J. Chem. Phys.* **1975**, *62*, 2469−2473.

(7) Beauchamp, R. N.; Gillies, C. W.; Craig, N. C. *J. Am. Chem. Soc.* **1987**, *109*, 1696−1701.

(8) Chiang, J. F.; Bernett, W. A. *Tetrahedron* **1971**, *27*, 975−980.

(9) Abdo, B. T.; Alberts, I. L.; Attfield, C. J.; Banks, R. E.; Blake, A. J.; Brain, P. T.; Cox, A. P.; Pulham, C. R.; Rankin, D. W. H.; Robertson, H. E.; Heppeler, A.; Murtagh, V.; Morrison, C. *J. Am. Chem. Soc.* **1996**, *118*, 209−216.

(10) Duncan, J. L.; Burns, G. R. *J. Mol. Spectrosc.* **1969**, *30*, 253−256.

(11) Baird, M. S.; Spencer, S. V.; Krasnoshchiokov, S. V.; Panchenko, Y. N.; Stepanov, N. F.; De Maré, G. R. *J. Phys. Chem. A* **1998**, *102*, 2363−2371.

(12) Craig, N. C.; Pranata, J. *J. Phys. Chem.* **1987**, *91*, 1764−1769.

(13) Craig, N. C.; Pranata, J.; Sprague, J. R.; Stevens, P. S. *Spectrochim. Acta* **1987**, *43A*, 753−761.

(14) Craig, N. C.; MacPhail, R. A.; Spiegel, D. A. *J. Phys. Chem.* **1978**, *82*, 1056−1070.16. Craig, N. C.; Fleming, G. F.; Pranata, J. *J. Phys. Chem.* **1985**, *89*, 100−105.

(15) Craig, N. C.; Alpern, J. K.; Parkin, K. M. *Spectrochim. Acta* **1975**, *31A*, 1463−1473.

(16) Craig, N. C.; Fleming, G. F.; Pranata, J. *J. Phys. Chem.* **1985**, *89*, 100−105.

(17) Craig, N. C.; Anderson, G. J.; Cuellar-Ferreira, E.; Koepke, J. W.; Martyn, P. H. *Spectrochim. Acta* **1972**, *28A*, 1175−1193.

(18) Craig, N. C.; Chao, T.-N. H.; Cuellar, E.; Hendriksen, D. E.; Koepke, J. W. *J. Phys. Chem.* **1975**, *79*, 2270−2282.

(19) Craig, N. C.; Pranata, J.; Reinganum, S. J.; Sprague, J. R.; Stevens, P. S. *J. Am. Chem. Soc.* **1986**, *108*, 4378−4386.

(20) Xie, Y.; Boggs, J. E. *J. Chem. Phys.* **1989**, *90*, 4320−4329.

(21) Xie, Y.; Boggs, J. E. *J. Chem. Phys.* **1989**, *91*, 1066−1071.

(22) Frisch, M. J.; Trucks, G. W.; Schlegel, H. B.; Scuseria, G. E.; Robb, M. A.; Cheeseman, J. R.; Montgomery, J. A., Jr.; Vreven, T.; Kudin, K. N.; Burant, J. C.; Millam, J. M.; Iyengar, S. S.; Tomasi, J.; Barone, V.; Mennucci, B.; Cossi, M.; Scalmani, G.; Rega, N.; Petersson, G. A.; Nakatsuji, H.; Hada, M.; Ehara, M.; Toyota, K.; Fukuda, R.; Hasegawa, J.; Ishida, M.; Nakajima, T.; Honda, Y.; Kitao, O.; Nakai, H.; Klene, M.; Li, X.; Knox, J. E.; Hratchian, H. P.; Cross, J. B.; Bakken, V.; Adamo, C.; Jaramillo, J.; Gomperts, R.; Stratmann, R. E.; Yazyev, O.; Austin, A. J.; Cammi, R.; Pomelli, C.; Ochterski, J. W.; Ayala, P. Y.; Morokuma, K.; Voth, G. A.; Salvador, P.; Dannenberg, J. J.; Zakrzewski, V. G.; Dapprich, S.; Daniels, A. D.; Strain, M. C.; Farkas, O.; Malick, D. K.; Rabuck, A. D.; Raghavachari, K.; Foresman, J. B.; Ortiz, J. V.; Cui, Q.; Baboul, A. G.; Clifford, S.; Cioslowski, J.; Stefanov, B. B.; Liu, G.; Liashenko, A.; Piskorz, P.; Komaromi, I.; Martin, R. L.; Fox, D. J.; Keith, T.; Al-Laham, M. A.; Peng, C. Y.; Nanayakkara, A.; Challacombe, M.; Gill, P. M. W.; Johnson, B.; Chen, W.; Wong, M. W.; Gonzalez, C.; Pople, J. A. *Gaussian 03*, revision C.02; Gaussian, Inc.: Wallingford, CT, 2004.

(23) Craig, N. C.; Anderson, G. J.; Cuellar-Ferreira, E.; Koepke, J. W.; Martyn, P. H. *Spectrochim. Acta* **1972**, *28A*, 1175−1193.

(24) Becke, A. D. *J. Chem. Phys.* **1993**, *98*, 5648−5652.

(25) Lee, C.; Yang, W.; Parr, R. G. *Phys. Rev. B* **1988**, *37*, 785−789.

(26) Dunning, T. H., Jr. *J. Chem. Phys.* **1989**, *90*, 1007−1023.

(27) Craig, N. C.; Groner, P.; McKean, D. C. *J. Phys. Chem. A* **2006**, *110*, 7461−7469.

(28) Groner, P.; Warren, R. D. *J. Mol. Struct.* **2001**, *599*, 323−335.

(29) Hedberg, L.; Mills, I. M. *J. Mol. Spectrosc.* **2000**, *203*, 82−95.

(30) STRFIT87 program came from Robert L. Kuczkowski's laboratory at the University of Michigan. The original program was written by Richard Schwendemann at Michigan State University.

(31) Werner, H.-J.; Knowles, P. J.; Lindh, R.; Manby, F. R.; Schütz, M.; Celani, P.; Korona, T.; Rauhut, G.; Amos, R. D.; Bernhardsson, A.; Berning, A.; Cooper, D. L.; Deegan, M. J. O.; Dobbyn, A. J.; Eckert, F.; Hampel, C.; Hetzer, G.; Lloyd, A. W.; McNicholas, S. J.; Meyer, W.; Mura, M. E.; Nicklass, A.; Palmieri, P.; Pitzer, R.; Schumann, U.; Stoll, H.; Stone, A. J.; Tarroni, R.; Thorsteinsson, T. *MOLPRO 2006.1;* Cardiff University: Cardiff, U.K., 2006 (http://www.molpro.net).

(32) Feller, D. *J. Chem. Phys.* **1992**, *96*, 6104−6114.

(33) Computed r_e structure for cyclopropane: $r_{CC} = 1.5024$ Å, $r_{CH} = 1.0791$ Å, $\alpha_{HCH} = 114.8°$ to give excellent agreement with the semi-experimental structure of $r_{CC} = 1.5030$ Å, $r_{CH} = 1.0786$ Å, $\alpha_{HCH} = 115.0°$ in ref 1.

(34) Feller, D.; Peterson, K. A. *J. Chem. Phys.* in press.